Temperature-Dependent Spin-Driven Dimerization Determines the Ultrafast Dynamics of a Copper(II)-Bound Tripyrrindione Radical

Anshu Kumar[αβ], *Benjamin Thompson*[αγ], *Ritika Gautam*[αζ], *Elisa Tomat*[α], *Vanessa Huxter**[αβ]

[α]Department of Chemistry and Biochemistry, University of Arizona, Tucson, Arizona 85721, United States

[β]Department of Physics, University of Arizona, Tucson, Arizona 85721, United States

[γ]Department of Optical Sciences, University of Arizona, Tucson, Arizona 85721, United States

[ζ]Present Address: Department of Chemistry, Indian Institute of Technology Kanpur, Kalyanpur, Kanpur, Uttar Pradesh 208016, India

Corresponding Author

*vhuxter@arizona.edu

ABSTRACT

Radicals and other open-shell molecules play a central role in chemical transformations and redox chemistry. While radicals are often highly reactive, stable radical systems are desirable for a range of potential applications ranging from materials chemistry and catalysis to spintronics and quantum information. Here we investigate the ultrafast properties of a stable radical system with temperature-dependent spin-tunable properties. This radical complex, Cu(II) hexaethyl tripyrrin-1,14-dione, accommodates unpaired electrons localized on both the copper metal center and on the tripyrrolic ligand. Two-dimensional electronic spectroscopy measurements of Cu(II) hexaethyl tripyrrin-1,14-dione were collected at room temperature and at 77 K. At room temperature, the molecules are present as monomers and have short, picosecond lifetimes. At 77 K, the molecules are present in a dimer form mediated by ferromagnetic and anti-ferromagnetic coupling. This reversible spin-driven dimerization changes the optical properties of the system, generating long-lived excitonic states.

TOC GRAPHIC

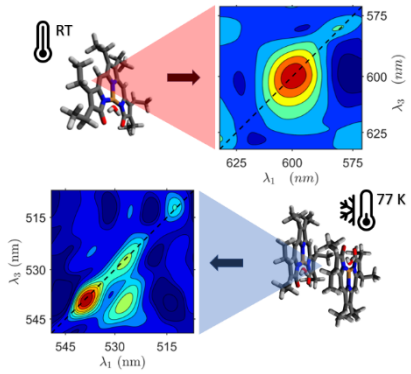

KEYWORDS Dimer; Dimerization; Radical; Ferromagnetic Coupling; Antiferromagnetic Coupling; 2DES; Ultrafast Spectroscopy.

Metal-bound radical systems are of particular interest for their ability to perform electron transfer and to enable chemical reactivity. They participate in a wide range of biological processes

including photosynthesis and enzyme catalysis. For example, the oxidization of alcohols by the fungal enzyme galactose oxidase is facilitated by a combination of a copper metal center and a tyrosine radical cofactor.[1, 2] In natural light harvesting, the oxidation of chlorophyll, a macrocyclic chlorin with phytyl chain bound to a magnesium metal center, generates a cationic radical that enables water splitting.[3-6] Complexes consisting of a transition metal center bound to organic ligands have been widely used in photoredox catalysis.[7-9] Following optical excitation, these systems can form highly reactive radicals that permit challenging chemical transformations without the use of harsh conditions.

In this paper we present the ultrafast dynamics of a stable neutral radical complex featuring both a ligand-based and a metal-based unpaired spin: a hexaethyl tripyrrin-1,14-dione radical bound to a Cu(II) center (i.e., [Cu(TD1$^{\bullet}$)(H_2O)], abbreviated TD1-Cu).[10-13] The square planar TD1-Cu complex, shown in Figure 1 (a), features a monodentate aqua ligand and a tridentate tripyrrindione, with an electron-rich planar π system capable of reversible one-electron oxidation and reduction chemistry that is of interest for catalytic and redox sensing applications. The neutral radical TD1-Cu complex has one unpaired electron formally in the π system of the tripyrrindione ligand and a

second unpaired electron associated with the d^9 copper center. These unpaired spins are in near-orthogonal orbitals, resulting in an overall triplet ground state.[11]

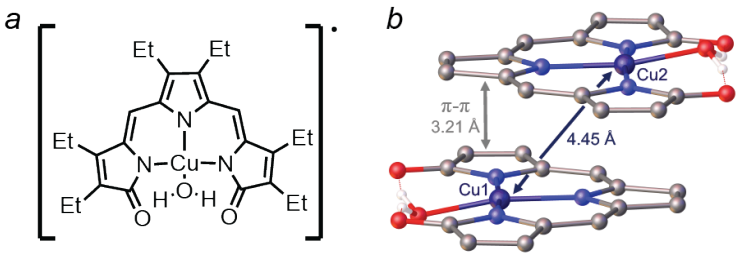

Figure 1. (a) Structure of TD1-Cu (i.e., [Cu(TD1•)(H2O)]) and (b) selected metrics of a representative π dimer observed in the crystal structure (CCDC 1496214). Carbon-bounds hydrogen atoms and ethyl substituents are omitted for clarity.

Recently, our group reported the ultrafast dynamics of TD1-Cu at room temperature using transient absorption spectroscopy. These studies showed that the lifetime of the excited state of the monomer biradical form of TD1-Cu was sub 20 picoseconds.[14] At low temperature, metal-bound tripyrrindione radicals reversibly form p stacked dimers, as shown in Figure 1 (b), mediated by multicenter interactions (also described as pancake bonding[15, 16]) and antiferromagnetic coupling between the unpaired electrons on the ligands.[11, 17, 18] In this paper, we use temperature-dependent two-dimensional electronic spectroscopy (2DES) to observe ultrafast dynamics of TD1-

Cu in its monomeric and dimeric forms. These measurements show that TD1-Cu forms excitonic dimers with long-lived excited states at low temperatures compared to the short excited-state lifetime of the room temperature radical monomer.

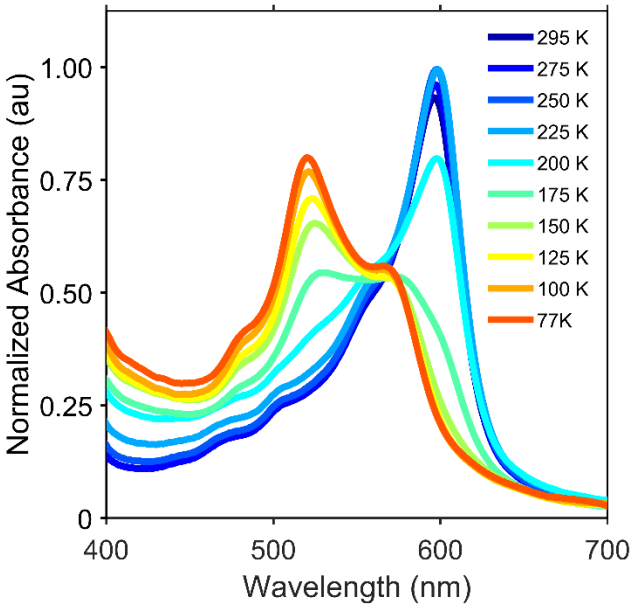

Figure 2. Steady-state absorption of TD1-Cu in a 6:1 v/v methylcyclohexane-toluene mixture, illustrating the temperature-dependent changes from 295 K to 77 K.

Figure 2 shows the temperature-dependent absorption spectrum of TD1-Cu in a methylcyclohexane:toluene mixture (6:1 volume ratio) from 295 K to 77 K. The steady-state absorption spectra were collected using an Agilent Cary 100. No fluorescence was observed for TD1-Cu in the monomer or the dimer form. In our previous work on TD1-Cu, we did not observe

any fluorescence at room temperature for either the neutral radical or the oxidized species.[14] The lack of fluorescence in TD1-Cu is unsurprising due to the existence of low-lying states that allow relaxation via radiationless transitions (energy gap law).[19,20,21] These low-lying states with very small oscillator strengths are characteristic of ligand-based radicals of oligopyrrole complexes and appear in the near IR region (see Figure S2 in the Supporting Information).

The 295 K absorption spectrum displays a prominent band in the visible region at 600 nm. These transitions originate from π to π* transitions[14] localized on the tripyrrindione ligand. As the temperature is lowered, the primary absorption peak in the visible shifts from 600 nm to 521 nm. This change in the absorption spectrum is associated with the formation of a dimer at low temperatures enabled in part by interactions between the unpaired electrons. In the monomer, the unpaired electron on the metal center is localized in the $d_{x^2-y^2}$ orbital, which is near orthogonal to the ligand's π orbitals that accommodate the other unpaired electron,[11,14] stabilizing the triplet ground state. Upon lowering the temperature, TD1-Cu undergoes a reversible dimerization process facilitated by antiferromagnetic coupling between the electrons localized on the ligand as well as ferromagnetic interactions between the electrons localized on the Cu(II) metal centers.[11] The presence of an isosbestic point implies the existence of two interconverting equilibrium

populations and is representative of the conversion of the monomer to the dimer. The peaks in the near-IR (Figure S2 in the Supporting Information) also shift and display isosbestic points consistent with dimerization involving a change in the local environment of the ligand-based electron.

The temperature-dependent absorption data was used to determine thermodynamic parameters for the dimerization process in the methylcyclohexane-toluene mixture. Assuming that the monomer and the dimer are the primary contributions to the absorption at 295K and 77 K respectively, relative absorption intensities were used to determine values for equilibrium constants and ΔG at different temperatures (additional information in Section 3 of the Supporting Information). The temperature dependence of ΔG (Figure S10 in the Supporting Information) was used to determine dimerization enthalpy and entropy changes. The values obtained, $\Delta H = -4.07 \pm 0.08$ kCal/mol and $\Delta S = -21.9 \pm 0.3$ Cal/mol·K, are consistent with previously published values.[11] Both ΔH and ΔS are negative, indicating that dimerization is spontaneous at low temperatures. The temperature at which ΔG switches from positive to negative is approximately 185 K. This is consistent with our steady-state absorption spectra, which show a significant change between the 200 K and 175 K traces.

Figure 3 (a)–(f) presents several representative 2DES spectra of TD1-Cu at room temperature. These spectra were acquired using a laser pulse centered at 600 nm, covering a spectral range of 570 nm to 633 nm. A brief description of the experimental setup is provided here (additional details can be found in Section 2 of the Supporting Information). The 2DES measurements were collected using a home-built femtosecond pump-probe geometry 2DES setup. A 1kHz regenerative-amplifier laser system, Coherent (Libra), was used to power a home-built single-pass noncolinear optical parametric amplifier (NOPA). The NOPA output was compressed using a prism compression line and later split to generate pump and probe pulses. The pump pulse was passed through a pulse shaper, FASTLITE Dazzler, to provide controllable variable time delay between two collinear pump pulses. This delay between the two pump pulses is called t_1 or the coherence time, and the delay between the pump pulses and the probe is called t_2 or the population time. The spot size of the pump and probe beams at the sample position was approximately 80 μm. The NOPA output was centered at 600 nm and 529 nm for the room temperature (295 K) and 77 K measurements respectively (see Figure S1 in the Supporting Information). Second harmonic generation signal generated with a BBO revealed a temporal width of sub-45 fs and sub-40 fs for the pulses used for the room temperature and 77 K measurements, respectively, which was

complemented by polarization gated frequency resolved optical gating (PG-FROG) using a non-resonant sample (see Figures S3 and S4 in the Supporting Information). After the sample position, the probe was focused onto a spectrometer (SpectraPro HRS-300) and detected on a CCD (PIXIS 400, Princeton Instruments). The detection frequency axis collected using the CCD corresponds to the λ_3 axis in the 2DES plots, the λ_1 axis is generated from the Fourier transform of the delay between the pump pulses t_1. Each 2DES plot corresponds to a single point along the population time, t_2.[22, 23]

In Figure 3, the strong feature that appears on the diagonal at 600 nm in panel (a) is associated with a ground state bleach (GSB) of the primary π to π* transition shown in the room temperature (295K) absorption spectrum (Figure 2).

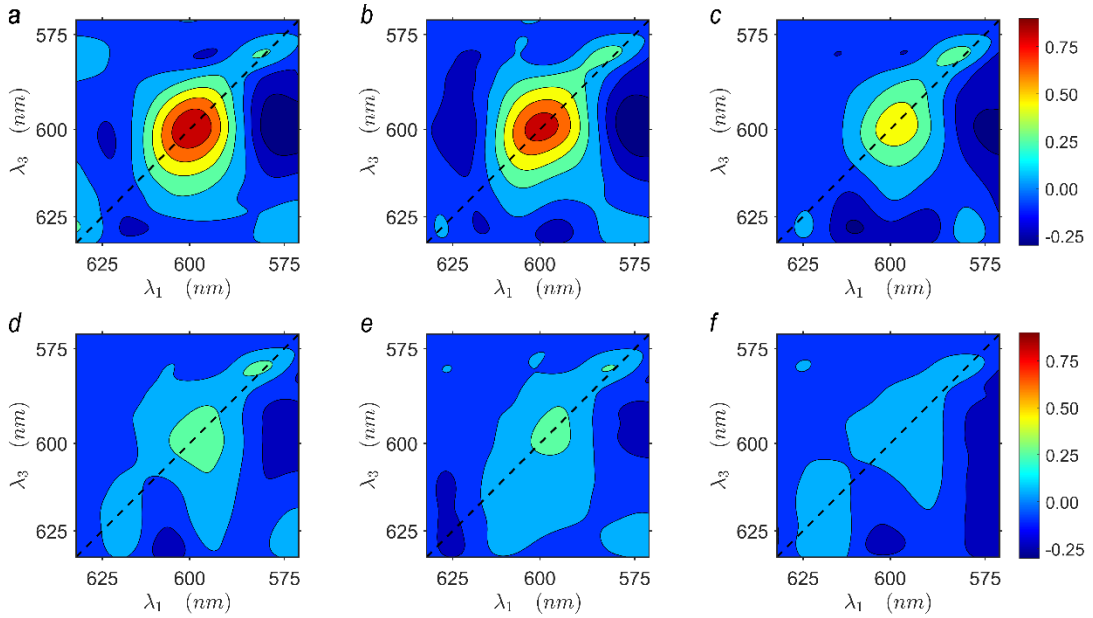

Figure 3. Representative absorptive 2DES surfaces for TD1-Cu at 295 K at various t_2 delay times: (a) 0.4 ps, (b) 1.2 ps, (c) 13 ps, (d) 30 ps, (e) 100 ps, (f) 400 ps.

A second ground state bleach (GSB) feature associated with an electronic transition at 581 nm appears on the diagonal in Figure 3 (see also Supporting Information Figure S5), coinciding with the shoulder observed in the 295 K absorption spectrum. However, due to its proximity to the edge of the laser spectrum, the associated signal is weak. In Figure 3 (b)-(d), an excited-state absorption (ESA) feature is observed as an off-diagonal peak at $\lambda_1 = 606$ nm and $\lambda_3 = 625$ nm. Although this signal is extremely weak, it exhibits a blue shift in its peak as the population time increases (Supporting Information Figure S6) consistent with our previous findings[14]. An off-diagonal ESA

peak is present at $\lambda_1 = 578$ nm and $\lambda_3 = 600$ nm associated with transitions to higher lying π states. This feature was hidden in our previous transient absorption measurements due to the large GSB at the same detection wavelength (λ_3) but appears in these 2DES spectra due to the resolution of the λ_1 axis. In addition, a positive feature associated with stimulated emission (SE) is observed along the diagonal at 622 nm (see also Supporting Information Figure S7). This feature was not observed in our previous transient absorption measurements due to the large ESA at the same detection wavelength (λ_3) but appears in these 2DES spectra due to the resolution of the λ_1 axis. We previously postulated the existence of a hidden SE feature in our previous work and this data shows that this feature indeed exists.

To determine the decay timescales associated with the diagonal 600 nm peak in Figure 3 (a)–(f), the associated region of the 2DES data was integrated (see also Supporting Information Figure S8) and plotted as a function of t_2 and fit to decaying exponentials. From these data, two timescales were recovered, 2.5 ± 0.4 ps and 13.8 ± 1.0 ps. These timescales are in agreement with our previously reported results for this system at room temperature[14], with the shorter timescale corresponding to vibrational relaxation and the longer timescale to the lifetime of the excited state.

Due to low signal, a reliable timescale could not be extracted from the ESA feature at $\lambda_1 = 606$ nm and $\lambda_3 = 625$ nm, however, that signal is also gone at long t_2 times.

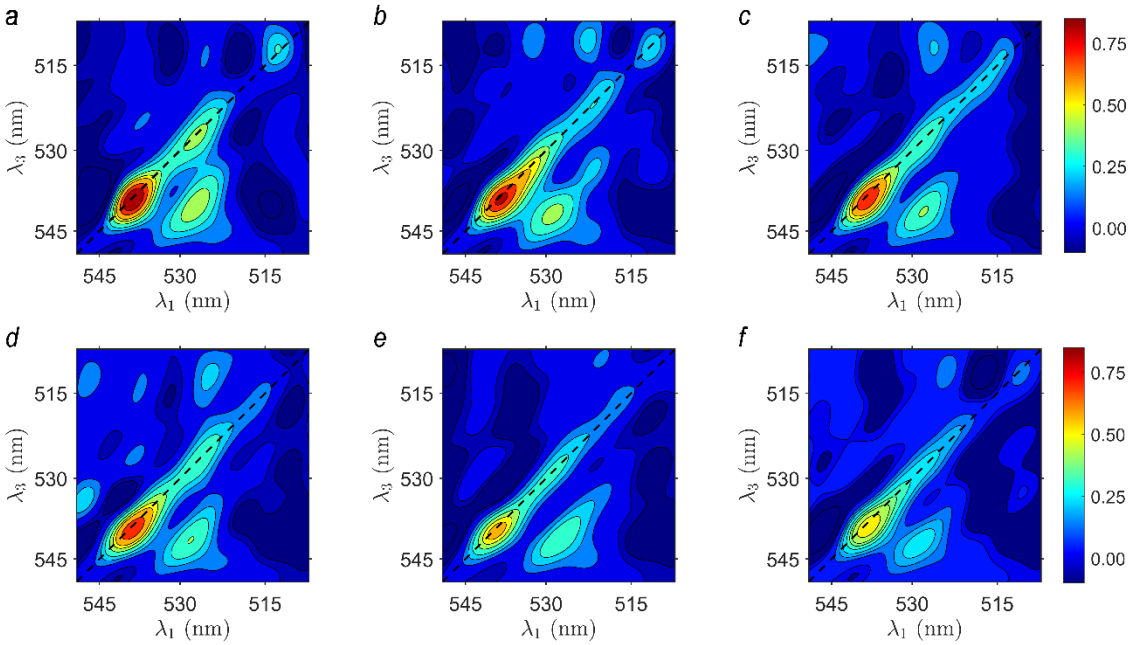

Figure 4. Representative absorptive 2DES surfaces for TD1-Cu at 77 K at various t_2 delay times: (a) 0.4 ps, (b) 1.2 ps, (c) 13 ps, (d) 30 ps, (e) 100 ps, (f) 400 ps.

The 2DES experiments at 77 K used a laser pulse with a central wavelength of 529 nm (see Supporting Information Figure S1). This pulse is overlapped with the primary absorption feature in the 77 K spectrum. As the spectral bandwidth of this pulse did not span the entire transition, there is some shaping of the features in the 2DES spectrum due to a convolution of the absorption with the laser pulse. This means that the maxima of the features in Figure 4 do not necessarily

correspond to the peaks of the transitions but correspond to the combination of the laser pulse and the spectra. Figure 4 (a)–(f) displays representative 2DES surfaces at 77 K for various t_2 delays. The change in temperature from 295 K to 77 K and the associated dimerization of TD1-Cu significantly changes the observed signal. At 295 K, the 2DES measurements are dominated by the GSB on the diagonal at 600 nm (Figure 3 (a)–(d)) and all features disappear on the order of tens of picoseconds. At 77 K, we observe two closely spaced narrow diagonal peaks at 528 nm and 539 nm (Figure 4 (a)–(f)). These correspond to GSBs from two excitonic energy levels. A crosspeak also appears at λ_1 = 528 nm and λ_3 = 539 nm, associated with energy transfer between the higher to the lower state. The crosspeak appears due to electronic coupling in the dimer. All features observed in the 2DES spectra at 77 K persist to the maximum experimental delay of 400 ps, while at 295 K, the signal has fully decayed within the first 100 ps, highlighting the presence of much longer-lived excited state in the TD1-Cu dimer compared to its room temperature monomer counterpart.

The two diagonal peaks at 539 nm and 528 nm in the 77 K 2DES spectra arise from the GSB of two closely positioned electronic transitions originating from the triplet ground state of the dimer. Based on EPR measurements,[11] the ligand spin in the dimer is quenched due to strong

antiferromagnetic coupling, while the spins on the Cu metal centers pair, resulting in a signal typical of a Cu(II) dimeric species with a spin triplet.[11] These GSB features are associated with the peak in the 77 K steady-state absorption spectrum (Figure 2) near 525 nm and a broad shoulder on the low energy side. The signal corresponding to these GSBs persists throughout the entire experimental delay of 400 ps. Notably, the off-diagonal crosspeak between these two states is present from the beginning of the experiment, providing evidence of strong excitonic coupling between these states. This crosspeak also persists beyond the maximum experimental delay.

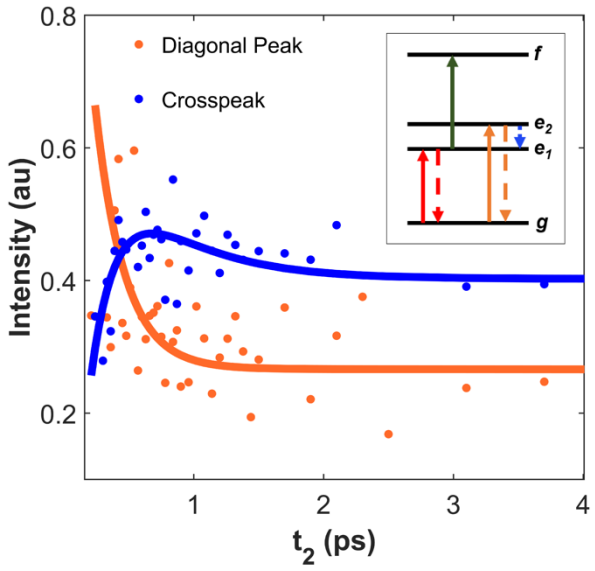

Figure 5. Short time dynamics for the 528 nm electronic transition and the crosspeak at $\lambda_1 = 528$ nm and $\lambda_3 = 539$ nm. The dots correspond to data points from integrated regions of the 2DES

spectra at delay times, t_2. The solid lines are fit with exponential terms reported in the main text. The inset presents the level structure for the dimer.

The decay timescales for the two diagonal peaks as well as the crosspeak in the 77 K 2DES data were determined by integrating the corresponding regions (Figure 5 and Figure S9) for all t_2 delay times. The integrated trace of the GSB at 528 nm has a biexponential decay with timescales of 240 ± 70 fs and 1.8 ns ± 300 ps. Similarly, the lower energy state at 539 nm also displays a biexponential decay profile with a fast decay component of 480 ± 60 fs, followed by a long timescale of 1.7 ns ± 500 ps. Unlike the diagonal features, the crosspeak signal rises during the early population times with a timescale of 165 ± 70 fs. The higher energy diagonal peak has a corresponding but oppositely signed sub-250 fs timescale. These timescales are associated with an energy transfer process between the two states resulting from excitonic coupling.[24] Following the rise in the signal from the fast energy transfer, the crosspeak then undergoes a biexponential decay with timescales of 460 ± 80 fs and 1.5 ns ± 300 ps. The 460 fs and 480 fs timescales observed for the crosspeak and the diagonal peak at 539 nm, respectively, correspond to vibrational relaxation in the lower energy transition.

Both diagonal peaks as well as the crosspeak in the 77 K data persist beyond the maximum delay of the experiment. In contrast, at room temperature, the lifetime of the excited state is on the order of tens of picoseconds. The significantly longer excited-state lifetime at low temperature means that the process facilitating fast (picosecond) excited-state relaxation in the monomer at 295 K is not available at 77 K due to a change in the electronic structure associated with dimerization. Fast excited-state decay in the monomer at 295 K is likely mediated through coupling to metal-centered states. Dimerization involves coupling between the spins localized on the copper metal centers and significantly modifies the electronic structure, as shown by the shift in the absorption spectra. This change in the electronic structure likely makes the 295 K deactivation pathway unfavorable and leading to longer-lived excited-state lifetimes.

The temperature-dependent change in the electronic structure arises from excitonic coupling in the dimer. At 77 K, the TD1-Cu dimer behaves like a model excitonic system. Upon dimerization, the resulting excitonic states, denoted as e_1 and e_2 in the inset in Figure 5, appear in the 77 K 2DES data at 539 nm and 528 nm, respectively. Up arrows signify transitions to higher energy electronic states, while down dashed arrows denote population relaxation to lower energy electronic states. The formation of an excitonic dimer at 77 K is supported by the observation of an energy transfer

crosspeak. We also see evidence of a weak diagonal peak at 514 nm in the 77 K 2DES data (Figure 4), which is associated with the doubly-excited state, denoted as *f* in Figure 5 inset. This peak is at the edge of our laser spectrum and, as a result has low signal. This state is populated through excitation of the population in the e_1 excitonic state and is not directly accessible via a single transition from the triplet ground state of the dimer. [25] Based on the thermodynamic parameters (Supporting Information Section 4 and Figure S10) recovered from our absorption data, ΔG of dimerization is equal to zero at approximately 185 K. Considering the value of kT at that temperature, the coupling interaction driving dimerization is approximately 16 meV. In addition, the average energy of excitonic states is blue-shifted by approximately 250 meV with respect to the ground state in the dimeric form in comparison to the energy difference between the excited state and ground state of the monomer. This shift in energy is an order of magnitude greater than the coupling interaction, as expected for molecular dimers.[24,26]

In conclusion, the temperature-dependent reversible spin-mediated dimerization of TD1-Cu modifies the optical properties, leading to significant changes in the electronic structure and the ultrafast dynamics. At room temperature, the triplet monomer form of TD1-Cu is a Cu(II)-bound radical whose excited state decays with a picosecond timescale. At 77 K, dimerization mediated

by spin interactions between unpaired electrons on each of the monomers results in an excitonic system with a long excited-state lifetime. These measurements demonstrate the spin-based temperature-switchable optical properties of TD1-Cu. These findings suggest that the TD1-Cu system may be useful as a spin- and temperature-controlled molecular switch with applications in areas ranging from spin dynamics to redox chemistry and catalysis.

ASSOCIATED CONTENT

Supporting Information. Details of the experimental methods, calculation of the thermodynamics parameters of dimerization, as well as supplemental spectroscopic data including steady-state absorption, pulse characterization, 2DES traces, and integrated data with corresponding fits.

AUTHOR INFORMATION

The authors declare no competing financial interests.

ACKNOWLEDGMENT

V. M. H. gratefully acknowledges support from the donors of the American Chemical Society Petroleum Research Fund through grant no. 65536-ND6 and from the National Science Foundation through CAREER award grant no. 2236610. E. T. gratefully acknowledges support from the National Science Foundation through grant CHE-2203361.

REFERENCES

(1) Himo, F.; Eriksson, L. A.; Maseras, F.; Siegbahn, P. E. M. Catalytic Mechanism of Galactose Oxidase: A Theoretical Study. *JACS* **2000**, *122* (33), 8031-8036.

(2) Chaudhuri, P.; Wieghardt, K.; Weyhermüller, T.; Paine, T. K.; Mukherjee, S.; Mukherjee, C. Biomimetic Metal-Radical Reactivity: Aerial Oxidation of Alcohols, Amines, Aminophenols and Catechols Catalyzed by Transition Metal Complexes. *Biol. Chem.* **2005**, *386* (10), 1023-1033.

(3) Capone, M.; Sirohiwal, A.; Aschi, M.; Pantazis, D. A.; Daidone, I. Alternative Fast and Slow Primary Charge-Separation Pathways in Photosystem II. *Angew. Chem. Int. Ed.* **2023**, *62* (16), e202216276.

(4) Yoneda, Y.; Arsenault, E. A.; Yang, S., Jr.; Orcutt, K.; Iwai, M.; Fleming, G. R. The Initial Charge Separation Step in Oxygenic Photosynthesis. *Nature Comm.* **2022**, *13* (1), 2275.

(5) Saito, K.; Ishida, T.; Sugiura, M.; Kawakami, K.; Umena, Y.; Kamiya, N.; Shen, J.-R.; Ishikita, H. Distribution of the Cationic State over the Chlorophyll Pair of the Photosystem II Reaction Center. *JACS* **2011**, *133* (36), 14379-14388.

(6) Narzi, D.; Bovi, D.; De Gaetano, P.; Guidoni, L. Dynamics of the Special Pair of Chlorophylls of Photosystem II. *JACS* **2016**, *138* (1), 257-264.

(7) Twilton, J.; Le, C.; Zhang, P.; Shaw, M. H.; Evans, R. W.; MacMillan, D. W. C. The Merger of Transition Metal and Photocatalysis. *Nature Rev. Chem.* **2017**, *1* (7), 0052.

(8) Huo, H.; Shen, X.; Wang, C.; Zhang, L.; Röse, P.; Chen, L.-A.; Harms, K.; Marsch, M.; Hilt, G.; Meggers, E. Asymmetric Photoredox Transition-Metal Catalysis Activated by Visible Light. *Nature* **2014**, *515* (7525), 100-103.

(9) Hopkinson, M. N.; Sahoo, B.; Li, J.-L.; Glorius, F. Dual Catalysis Sees the Light: Combining Photoredox with Organo-, Acid, and Transition-Metal Catalysis. *Chem. Eur. J* **2014**, *20* (14), 3874-3886.

(10) Bahnmüller, S.; Plotzitzka, J.; Baabe, D.; Cordes, B.; Menzel, D.; Schartz, K.; Schweyen, P.; Wicht, R.; Bröring, M. Hexaethyltripyrrindione (H_3Et_6tpd): A Non-Innocent Ligand Forming Stable Radical Complexes with Divalent Transition-Metal Ions. *Eur. J. Inorg. Chem* **2016**, *2016* (29), 4761-4768.

(11) Gautam, R.; Astashkin, A. V.; Chang, T. M.; Shearer, J.; Tomat, E. Interactions of Metal-Based and Ligand-Based Electronic Spins in Neutral Tripyrrindione π Dimers. *Inorg. Chem.* **2017**, *56* (11), 6755-6762.

(12) Tomat, E. Coordination Chemistry of Linear Tripyrroles: Promises and Perils. *Comments on Inorganic Chemistry* **2016**, *36* (6), 327-342.

(13) Tomat, E.; Curtis, C. J. Biopyrrin Pigments: From Heme Metabolites to Redox-Active Ligands and Luminescent Radicals. *Acc. Chem. Res.* **2021**, *54* (24), 4584-4594.

(14) Cho, B.; Swain, A.; Gautam, R.; Tomat, E.; Huxter, V. M. Time-Resolved Dynamics of Stable Open- and Closed-Shell Neutral Radical and Oxidized Tripyrrindione Complexes. *Phys. Chem. Chem. Phys.* **2022**, *24* (26), 15718-15725.

(15) Preuss, K. E. Pancake Bonds: π-Stacked Dimers of Organic and Light-Atom Radicals. *Polyhedron* **2014**, *79*, 1-15.

(16) Kertesz, M. Pancake Bonding: An Unusual Pi-Stacking Interaction. *Chem. Eur. J* **2019**, *25* (2), 400-416.

(17) Tomat, E.; Curtis, C. J.; Astashkin, A. V.; Conradie, J.; Ghosh, A. Multicenter Interactions and Ligand Field Effects in Platinum(II) Tripyrrindione Radicals. *Dalton Trans.* **2023**, *52* (19), 6559-6568.

(18) Habenšus, I.; Ghavam, A.; Curtis, C. J.; Astashkin, A. V.; Tomat, E. Primary Amines as Ligands and Linkers in Complexes of Tripyrrindione Radicals. *J. Porphyr. Phthalocyanines.* **2023**, *27*, 1448-1456.

(19) Englman, R.; Jortner, J. The Energy Gap Law for Radiationless Transitions in Large Molecules. *Mol. Phys.* **1970**, *18* (2), 145-164.

(20) Gouterman, M. Optical Spectra and Electronic Structure of Porphyrins and Related Rings. In *The Porphyrins*, Vol. 3; 1978.

(21) Straub, K. D.; Rentzepis, P. M.; Huppert, D. Picosecond Spectroscopy of Some Metalloporphyrins. *J. Photochem.* **1981**, *17* (2), 419-425.

(22) Biswas, S.; Kim, J.; Zhang, X.; Scholes, G. D. Coherent Two-Dimensional and Broadband Electronic Spectroscopies. *Chem. Rev.* **2022**, *122* (3), 4257-4321.

(23) Fuller, F. D.; Ogilvie, J. P. Experimental Implementations of Two-Dimensional Fourier Transform Electronic Spectroscopy. *Ann. Rev. Phys. Chem.* **2015**, *66* (1), 667-690.

(24) Van Amerongen, H.; Van Grondelle, R. *Photosynthetic Excitons*; World Scientific, 2000.

(25) do Casal, M. T.; Toldo, J. M.; Barbatti, M.; Plasser, F. Classification of Doubly Excited Molecular Electronic States. *Chem. Sci.* **2023**, *14* (15), 4012-4026.

(26) Silinsh, E. A.; Cápek, V. *Organic Molecular Crystals: Interaction, Localization, and Transport Phenomena*; 1994.